Available online at www.sciencedirect.com

jmr&t Journal of Materials Research and Technology

journal homepage: www.elsevier.com/locate/jmrt

Original Article

Effects of gradient distribution and aggregate structure of fibers on the flexibility and flexural toughness of natural moso bamboo (*Phyllostachys edulis*)

Xin Wei [a,b], *Ge Wang* [a,*], *Lee Miller Smith* [c], *Xiaoyi Chen* [a,b], *Huan Jiang* [a,b]

[a] *International Center for Bamboo and Rattan, Beijing, 100102, China*
[b] *Key Laboratory of National Forestry and Grassland Administration/Beijing for Bamboo & Rattan Science and Technology, Beijing, 100102, China*
[c] *Mechanical and Energy Engineering, University of North Texas (UNT), Denton, TX, 76203, USA*

ARTICLE INFO

Article history:
Received 25 October 2021
Accepted 14 December 2021
Available online 17 December 2021

Keywords:
Bamboo
Flexibility
Flexural toughness
Gradient distribution
Aggregate structure
Vascular bundles

ABSTRACT

Bamboo is a unidirectional fiber-reinforced material with excellent flexibility and flexural toughness arising from its unique cellular hierarchical structure, which creates an urgent demand in the bamboo industry to understand potential mechanisms of those two performances. In this study, a proposed original method was used to quantitatively evaluate the gradient distribution and aggregate structure of fibers on the flexibility and flexural toughness of natural moso (*Phyllostachys edulis*) bamboo, with a comparison to two other natural wood. Results showed that gradient distribution of fibers across the bamboo culm is the key to bamboo's varying flexibility along the diameter at the tissue level, whereas the asymmetric aggregate structure (vascular bundles) of fibers causes a difference in the flexibility when under different bending directions. Bamboo had possessed high strength and high toughness, but a conflict between the flexibility and flexural toughness existed. Compared to natural wood species of similar density, the flexibility and flexural toughness of bamboo was ~1.8 and 1.42–4.96 times greater that of wood, respectively. At the cell level, the combination of high-performance hard fibers and soft foamy parenchyma cells act upon the bamboo's flexibility, while the excellent flexural toughness stemmed from the fiber bridging and pull-out caused by high performance and aspect ratio, low microfibrils angle of fibers, and crack deflection along the longitudinal/radial direction. These findings helped contribute critical knowledge surrounding the flexibility and flexural toughness of bamboo, especially for optimizing the process of bamboo-based winding composites pipes (BWCPs).

* Corresponding author.
E-mail address: wangge@icbr.ac.cn (G. Wang).

https://doi.org/10.1016/j.jmrt.2021.12.071

1. Introduction

Bamboo is a collection of various large Gramineae plant species, which has been used as a material for pulp and paper, furniture, and engineering structures due to it being an abundant sustainable natural resource with high mechanical properties; all these attributes of bamboo make it a sustainable substitute for wood in regions where there is scarcity of forestry resources [1–3]. Bamboo exhibits excellent flexibility and flexural toughness in the axial direction due to its hierarchical cells structure (Fig. 1a); which endows it with the ability to withstand lateral wind, large deformation from load caused by snow, and prohibit crack growth when macrocracks occur during the growth of bamboo [4–6]. Besides traditional weaving crafts and textile products, bamboo can be used to manufacture advanced composite materials using advanced mold making processes and winding technologies [7], such as bamboo-based winding composites pipes (BWCPs) in Fig. 1b [8], bamboo motorcycle helmet [9], and interior automotive parts [10]. Therefore, by understanding bamboo's mechanical behavior at the microstructures especially the underlying mechanism of its flexibility and flexural toughness, it will improve the ability to fully tap into the potential of bamboo for new engineered applications.

Understanding the relationship between the mechanical performance of bamboo and its cell structure at the tissue to micro level has garnered considerable attention of late because of the impact it will have bamboo application [11–13]. At the tissue level, the mechanical properties of bamboo originate from the composition and distribution of the foam-like parenchyma tissues and vascular bundles (Fig. 1a), which provides compressibility and rigidity separately [14,15]. Of the two types of tissue at the tissue level, the vascular bundle consists of vessels and sieve tubes surrounded by fiber sheaths, the vascular bundle's shape can be divided into four main types according to Grosser and Liese [16]. Based on these four classification types of the vascular bundle their relaxation property, bending flexibility, and capacity absorption in relation to the shape were studied [17–19]. The volume fraction of the vascular bundles gradually increases from the internal side to the external side of the bamboo culm, from which the gradient of the mechanical properties was derived through experimental testing, mechanical model fitting, and finite element analysis [20–22]. However, to current knowledge, no reports have focused on the relationship between the anatomical structure and gradient distribution of vascular bundles on the flexibility and flexural toughness of bamboo at the tissue level.

According to published research, few studies have evaluated the influence that the factors of flexibility and flexural toughness have at the micro-cell level; which include the arrangement pattern, morphology, and mechanical properties of bamboo cells [23–25]. Obataya et al. [11] believed that the perfect combination of stretch-resistant fibers and compressible parenchyma cells was the key to bamboo's excellent flexible deformation. Chen et al. [26] initially illustrated the elongation of parenchyma cells under bending through low-resolution electron micrographs. Wang et al. [27] found that the microfibril angle (MFA) in the cell wall played an important role in the mechanical properties of the poplar wood. In a different study, Chen et al. [28] showed that when interfacial delamination occurred it was followed by matrix failure and fiber breakage under natural loading mode. Wang et al. [29] demonstrated that bamboo's excellent damage tolerance can be mainly attributed to the interplay between crack deflection and interfacial debonding at the cell-wall level. Through these studies a profound understanding of the flexibility and flexural toughness of bamboo at the tissue, micro-cell, and even cell-wall level can be achieved.

The aim of this study is to quantitatively investigate the effect of the gradient distribution and anatomical structure

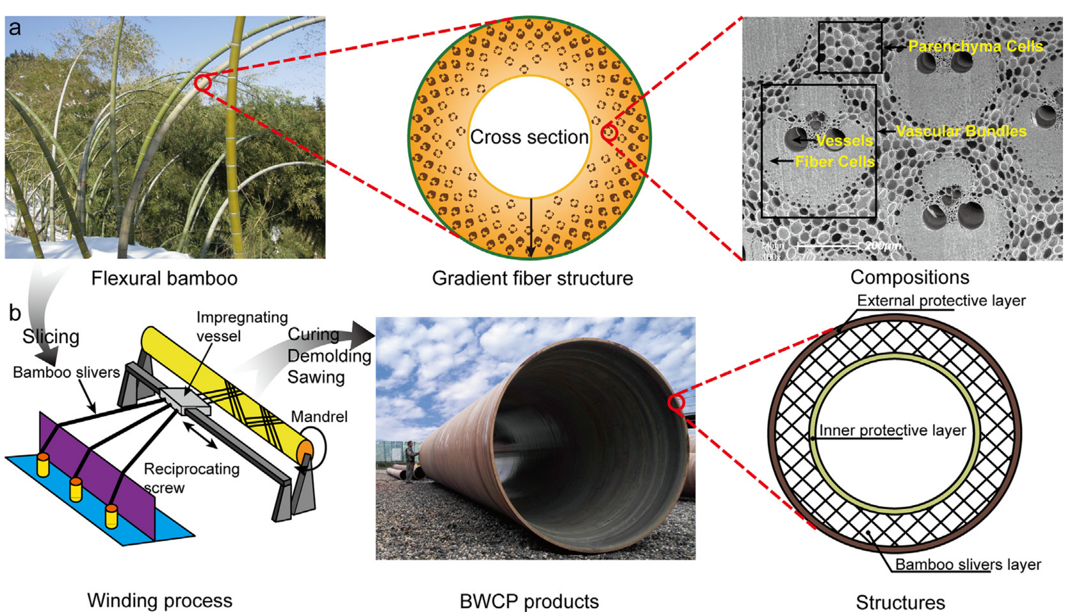

Fig. 1 – (a) Hierarchical structure of bamboo cells at different length scales; (b) Manufacturing, products, and structures of bamboo-based winding composites pipes (BWCPs) based on bamboo slivers.

of vascular bundles on the flexibility and flexural toughness of moso bamboo (*Phyllostachys edulis*) using a three-point bending test method. The microstructural differences and toughening mechanisms of bamboo were compared to two wood species used as a control, a low-density poplar (*Populus* spp.) and a high-density wood *Betula alnoides*; which were analyzed using a mechanical and energy dissipation model.

2. Materials and methods

2.1. Materials

4-year-old mature moso bamboo (*P. edulis*), was collected from a bamboo plantation located in Fujian Province in China, was selected as the raw material used for this study. The bamboo culm cut from the raw material was selected for being straight and defect-free (about 2 m above the ground for stable mechanical performance), which was then processed into bamboo strips (240 × 16 × 8 mm^3) by sawing and splitting. Considering its gradient fibers structure on the cross section, the bamboo strip was divided into 3 layers (240 × 16 × 1 mm^3) from the inner (IB), middle (MB), and outer (OB) bamboo layers, after which each layer was cut into 18 bamboo slivers (40 × 5 × 1 mm^3) for testing (Fig. 2a). According to Wei et al. [18], the cross-section of bamboo slivers was taken by a stereoscopic Lumenera INFINITY3-6URC microscope, and the fiber volume fraction (V_f) of 3 layers were calculated using Image Pro Plus (IPP) 6.0 graphics processing software (Media Cybernetics, Maryland, USA).

In order to eliminate the influence of size factors, the poplar (*Populus* spp.) wood (PW) and Birch (*B. alnoides*) wood (BW) were selected as a control group that possessed the same age, sampling position and size as the raw bamboo. All samples were adjusted to a moisture content of about 10% in a constant temperature and humidity chamber with 20 ± 2 °C and 65 ± 5% RH [22].

2.2. Flexural and fracture behaviors characterization

The flexural and fracture behavior of bamboo slivers under different loading types were tested using a Instron Microtester (5848, Instron Corporation, USA) to perform a 3-point bending test (Fig. 2b) with a load cell of 2 KN, span thickness ratio of 20, and loading rate of 2 mm/min in a test environment of 20 ± 2 °C and 65 ± 5% RH. Two forms of bending occurred in bamboo slivers in accordance to the shape of vascular bundles: loading on the side of the bamboo sliver that comes from the internal side of the bamboo culm (Type I) and loading on the outer side (Type II), both of which affect the flexural mechanical performance of bamboo slivers. The mechanical properties of the 3 layers were determined from the flexural stress–strain curves of the sliver samples (Fig. 2c) using the following formulas:

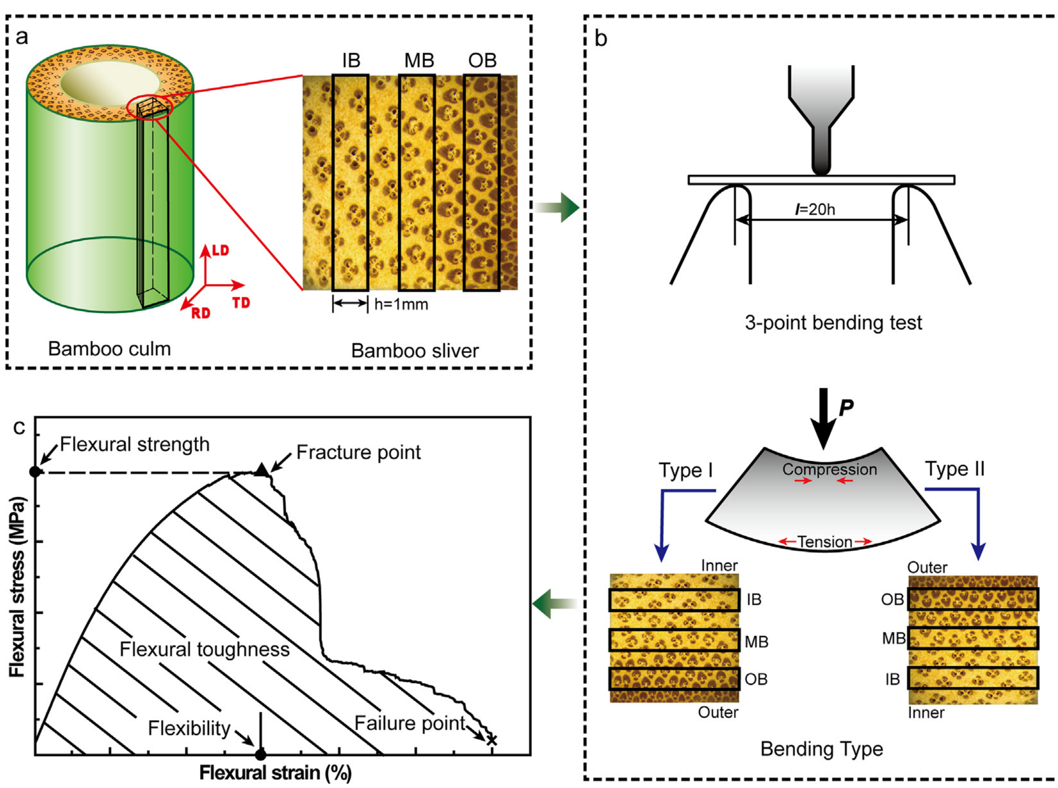

Fig. 2 – (a) Schematic diagram of the preparation of bamboo slivers samples; (b) the 3-point bending test under the outside tension (Type I) and the inside tension (Type II) at the bottom of different layer; c the typical flexural stress–strain curve of bamboo slivers. Flexibility is expressed by the flexural strain corresponding to the fracture point (mark as ▲), whereas the flexural toughness is calculated by integral area under the flexural stress–strain curve up to the complete failure point (cross symbol (×)).

$$E_f = kl^3 / 4bh^3 \quad (1)$$

$$\sigma_{max} = 3Pl / 2bh^2 \quad (2)$$

$$F = \varepsilon_{fra} = 6Dd / l^2 \quad (3)$$

$$T = \int_0^{\varepsilon_{fai}} \sigma(\varepsilon) d\varepsilon \quad (4)$$

The flexural modulus E_f and strength σ_{max} was calculated using the linear portion of the load–displacement curve and maximum load (*P*), respectively, along with length *l*, width *b*, and thickness *h*. Flexibility (*F*) also defined as flexural strain at fracture point (ε_{fra}), was calculated using the maximum deflection (*D*) of the samples. The flexural toughness (*T*) is an integral area of stress ($\sigma(\varepsilon)d\varepsilon$) on strain up to the complete failure point (ε_{fai}).

2.3. Fracture morphologies observation

The fracture morphologies of the bamboo slivers were observed with an optical microscope (SGO-67T1, KWONG KUK Optical Instrument, China) and a field-emission environmental scanning electron microscope (FESEM, XL30ESEM-FEG, FEI, USA), at a vacuum of 5.0×10^{-5} Pa and an acceleration voltage of 7 kV. The hairy morphology composed of fiber (peak) and matrix (base) in the SEM picture (Fig. 7b and d view) for bamboo slivers was outlined by IPP software, and the average pull-out length of the fiber was determined to the average height of the mountain—the area of the 'mountain' divided by the base.

2.4. Microfibril angle (MFA) measurement

The MFA of the bamboo, poplar wood (PW) and Birch wood (BW) were tested with an X-ray diffractometer (XRD) (X'Pert Pro, Panalytical, Netherlands) at voltage 40 KV, current 40 mA, and with a sample size of $40 \times 10 \times 1$ mm^3 (L × T × R). Each sample was attached to a holder in a hole (30 mm diameter) to ensure that the incident beam passed through the LT surface of the sample perpendicularly at a receiving light path of 22.4°. The rotation angle was set to 0°–360° with a scanning step of 0.5°. The XRD patterns were obtained with crystal face (002) diffraction with the strongest diffraction intensity. The average MFA was calculated according to the 0.6 *T* method (Eqs. (5) and (6)) developed by Cave [30]. Each group of samples was characterized 3 times.

$$y = a + b_1 e^{-\frac{(x-c)^2}{2w_1^2}} + b_2 e^{-\frac{(x-c-180)^2}{2w_2^2}} \quad (5)$$

$$\overline{MFA} = 0.6T = 0.6(w_1 + w_2) \quad (6)$$

where y is the diffraction intensity; a is a constant; b_1 and b_2 are the heights of peak centers c and c+180, respectively; The average microfibril angle ($\overline{MFA}$) was calculated using the 0.6T method which is the sum of the fitting parameters w_1 and w_2.

3. Results and discussion

3.1. Flexural behavior of bamboo

3.1.1. Gradient flexibility and flexural toughness

Due to the gradient distribution of fibers along the thickness of the bamboo culm, it was observed that the bamboo slivers prepared from different layers exhibited a gradient of flexibility and flexural toughness (in Fig. 3a and Table 1).

Consistent with the tension state of the outer surface of bamboo when under a lateral winding load, the Type I stress–strain curves were used to analyze the flexural and fracture behavior of bamboo (Fig. 3a). All of the curves were divided into two parts by flexural strain at the fracture point (εfra) (marked with a filled triangle in Fig. 3a), which was defined as the flexibility (*F*) of bamboo. Before fracture, the samples went through the linear elastic range followed by plastic range, after which they gradually reached maximum stress. Then, there was a plateau which was followed by a declining region with small peaks that looked like fine serrations. At the endpoint of the serrations regions was defined by the complete failure point (denoted by a red ×), which was used to calculate the flexural toughness (*T*). The existence of plateau was due to fibers bearing a continuous tensile load after the formation of macroscopic cracks in the matrix, which the fine serrations represent the debonding, fracture and pull-out of fibers that occur up to failure.

The flexural behavior characterization demonstrated that the OB possessed higher fiber volume fraction (V_f = 40.4%), exhibited lower *F* (2.42%) (Fig. 3c). However, as the location of sample collection approached the inner layers of the bamboo culm, their *F* increased to 2.49% with V_f of 14.6%. This means that the inner slivers possessed higher flexibility than the outer ones. The softer texture of the IB along with their stiff fibers of lower vascular bundle content and higher soft parenchyma cells generally causes larger deformation therefore making internal slivers more flexible. Opposite to the changing trend of *F*, the *T* of the OB gradually increased to 5.11×10^6 J m^{-3} from the 2.30×10^6 J m^{-3} of IB, which was derived from the interactive effects caused by the strengthening and toughening of higher fibers contents [11,31]. Specifically, the strengthening was mainly achieved through intrinsic toughening at the nanoscale, which limited the uncoiling of cellulose chains and intermolecular slippage; while the toughening was derived from the bridging and pull-out of fibers, which resulted in crack deflection on the macroscale. In addition, the changing pattern of the *T* with fiber content was similar to that of the fracture toughness, which increased with the increase in fiber content and decrease in parenchyma matrix content [32,33].

3.1.2. Asymmetric flexibility and flexural toughness

The aggregate structure (vascular bundles) of fibers though not as obvious as "its gradient distribution", is equally as important for the asymmetric flexibility and flexural toughness of bamboo.

The asymmetric flexural behavior of the same specimen can be compared from the flexural stress–strain curves under different bending configuration (Fig. 3b, and Table 1). The

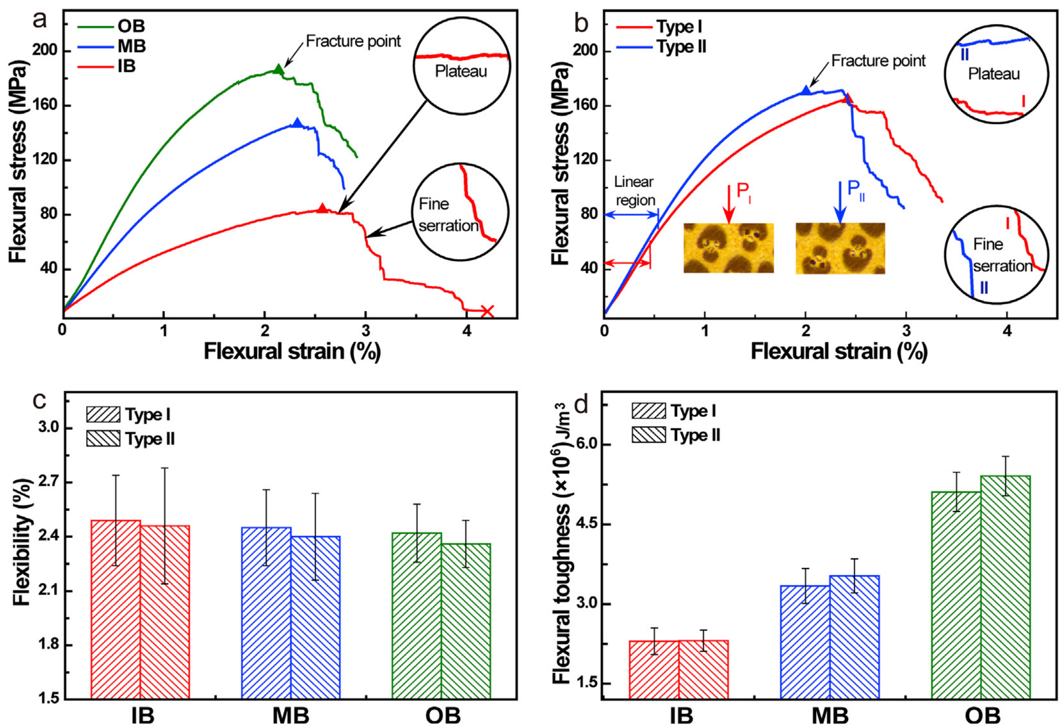

Fig. 3 – (a) The typical flexural stress–strain curves of bamboo sliver for 3 layers under Type I; (b) the comparison of typical flexural curve for the same layer under Type I and II, taking the outer bamboo (OB) layer as an example; (c) the flexibility and (d) flexural toughness of different layer from the inner to outer under Type I and Type II.

representative Type I curve of the outer layer (OB as an example) exhibited a relatively narrower linear region and wider elastoplastic region up to the fracture point, whereas the Type II showed the opposite phenomenon with wider linear region and lower flexural strain. After fracture, both Types exhibited a plateau at the peak with a similar length; but the Type I decreased at a slower rate followed by more serrations compared to the Type II, which implied that loading status in a natural environment (Type I) could delay the failure of the bamboo. Therefore, by cutting bamboo strips into slivers, the differences in the slivers when subjected to two different bending configurations could reveal the relationship between the anatomical structure of vascular bundles (fibers aggregate) and the flexural behavior, which is responsible for the asymmetric flexibility and flexural toughness.

With the same V_f of 40.4%, the OB layer under Type II bending exhibited higher mechanical performance and T (5.41×10^6 J m^{-3}) with lower F (2.36%) compared to Type I, which verified that bamboo in the outer layer could overcome the conflicts of between the strength and toughness [34] (Table 1). The difference of F and T under the two Types of bending gradually disappeared when the layers that the samples were taken from approach the inner layer of the bamboo culm (Fig. 3d). In previous studies, it was inclined that

Table 1 – Physical and flexural properties of bamboo slivers from the inner and outer layers subjected to different bending Types.

Bamboo slivers	Air-dried density (ρ) (g·cm-3)	Fiber volume fraction (V_f) (%)	Bending Types	Flexural modulus (E) (GPa)	Flexural strength (σ) (MPa)	Flexibility (F) (%)	Flexural toughness (T) (10^6 J·m^{-3})
IB	0.57 ± 0.02^a	14.6 ± 1.8^a	I	6.0 ± 0.6^a	94 ± 7^a	2.49 ± 0.25^a	2.30 ± 0.25^a
			II	6.0 ± 0.6^a	95 ± 8^a	2.46 ± 0.32^a	2.31 ± 0.20^a
MB	0.64 ± 0.03^b	25.0 ± 2.4^b	I	8.9 ± 1.2^b	135 ± 15^b	2.45 ± 0.21^a	3.34 ± 0.33^b
			II	9.0 ± 1.5^b	137 ± 16^b	2.40 ± 0.24^a	3.53 ± 0.32^b
OB	0.77 ± 0.03^c	40.4 ± 3.2^c	I	13.0 ± 1.5^c	188 ± 17^c	2.42 ± 0.16^a	5.11 ± 0.37^c
			II	14.0 ± 1.2^c	202 ± 11^c	2.36 ± 0.13^a	5.41 ± 0.37^c
BW	0.77 ± 0.03^c	/	/	13.5 ± 0.8^c	148 ± 7^d	1.38 ± 0.07^b	1.56 ± 0.15^d
PW	0.40 ± 0.02^d	/	/	7.6 ± 0.4^d	64 ± 6^e	1.67 ± 0.19^c	1.09 ± 0.18^e

Mean values ± standard deviation.
a, b, c, d, e Different letters in the same column indicate significant differences ($p < 0.05$).

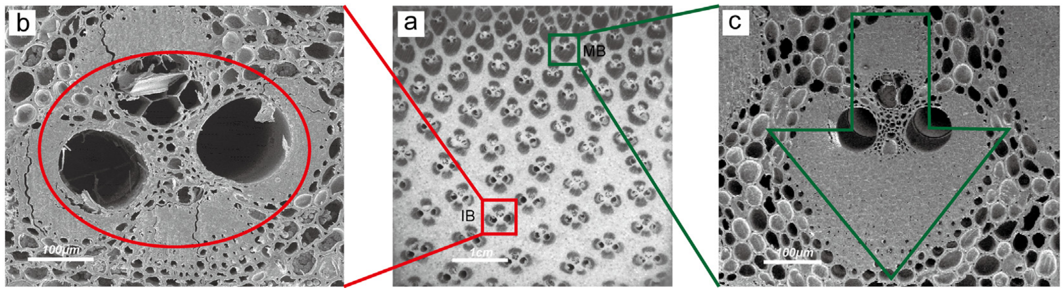

Fig. 4 – (a) The optical image of graded structure of vascular bundles (fibers aggregate) on bamboo culm cross section; The vascular bundles anatomically evolved into the (b) symmetrical "open" structure in the inner from the (c) arrow-shaped "semi-open" structure in the outer, which caused differences in mechanical properties of OB/IB layers at bending Type I and Type II.

the difference between the *F* and *T* can be attributed to the gradient distribution of vascular bundles [28,31]. However, by eliminating the gradient nature of the bamboo by using only thin bamboo slivers with only one layer of vascular bundle, a difference under different loading modes was still present. By observing the cross section of the bamboo culm, the anatomical shape of the vascular bundle showed the shape did have a specific orientation (Fig. 4a). The IB had four similarly sized and substantially symmetrical fibers aggregate formed an approximately elliptical vascular bundle which is called the "open" anatomy structure (Fig. 4b) [35], which was the cause for the IB having similar flexural performance under the two types of bending. The higher difference for OB was due to the "semi-open" arrow structure of the vascular bundles which are made up of two fibers sheaths, which results in more the fibers in the arrow head shape of the vascular bundles being in tension when under Type II bending when compared with the Type I (Fig. 4c). The purpose of the aggregate structure of fibers is to allow bamboo to overcome harsh environmental conditions by sacrificing a small amount of strength and stiffness to achieve greater flexural strain.

3.2. *Relationship between strength/flexibility and flexural toughness*

The plots of the relationship between strength and toughness in bamboo for both bending types bending indicated that the flexural toughness increased with an increase in strength, and there was a high correlation between the two properties ($R_{I}^{2} = 0.989$ and $R_{II}^{2} = 0.999$) (Fig. 5a). As such, bamboo as a material seems to overcome the general behavior of composites where a conflict exits between strength and toughness [36]. The high fiber content in the bamboo's outer layer bore most of the stress applied on the parenchyma cells matrix due to stress transfer that occurred at the interface and the high mechanical properties of the overall bamboo resisted external loads and deformations up until fracture. On the other hand, similar to other fiber-reinforced composites [37], it is also possible that the extrinsic toughening mechanisms that fiber bridging, pull-out, and cracks deflection/twist for shielding local stresses or strains acting at larger length scales and mostly behind the crack tip.

In both bending configurations, the there was a negative trend with high correlation between *F* and *T* ($R_{I}^{2} = 0.846$ and $R_{II}^{2} = 0.943$) (Fig. 5b). Bamboo is a typical soft-hard natural composite material where hard fibers are embedded in soft foamy parenchyma cells matrixes, like bone and nacre [38]. The high-content hard fibers in bamboo's outer layer affects the properties at the interface of the fibers/parenchyma cells; which restricts slipping at the interface and ultimately causes the whole material to be more rigid and inflexible. These findings about in bamboo are consistent with Lu's research [39] on metals. Stronger metals have higher tensile strain through the gradient distribution of the crystal grain sizes, which increase from nanoscale at the surface to coarse-grained in the core.

This unique consensus and conflicting property are very meaningful for the biological simulation. By Imitating the hollow structure of bamboo with the gradient structure of the fibers in the culm, the optimization of BWCPs processing can become possible: the use of the inner bamboo slivers which possess larger flexibility and lower mechanical performance can be wrapped around a mandrel to function as the inner layer whereas the outer layer of slivers would be used to make a rigid outer layer of BWCPs. Instead of using the existing process of non-uniform winding that chaotically and disorderly puts bamboo slivers from different layers of the gradient structure a more uniform method of winding can be done. At the same time, this proposed process demonstrates that understanding and analyzing the gradient structure of bamboo can help to optimize the mechanical properties and achieved excellent flexural behavior of industrial bamboo product applications such as BWCPs, while preventing breakage from extreme external loads.

3.3. *Comparison between bamboo and wood*

3.3.1. *Comparison on flexural behavior*

Compared to the OB, the BW which possessed a similar density (0.77 g cm^{-3}) exhibited a relatively brittle behavior for a high-modulus material, where fracture occurred suddenly with little nonlinear deformation (Fig. 6a). After fracture, BW failed quickly, which resulted in lower toughness. The same phenomenon also occurred between the IB and the PW.

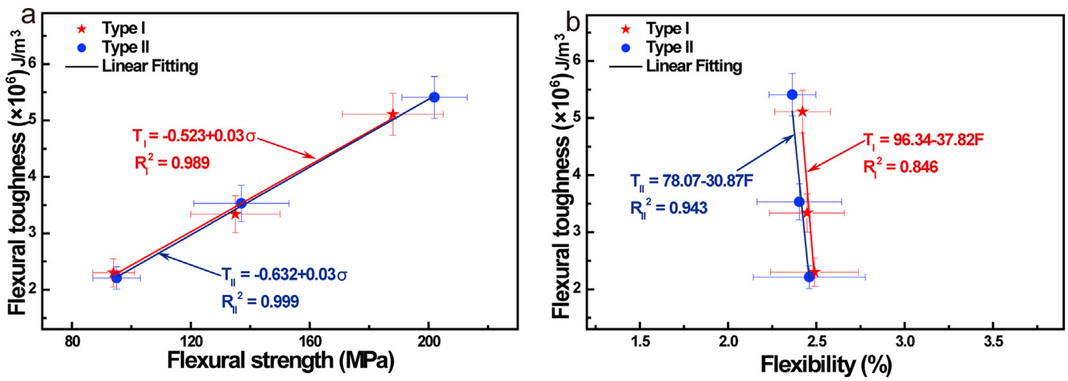

Fig. 5 – (a) Relationship between flexural strength and flexural toughness; (b) Relationship between flexibility and flexural toughness.

Specifically, the low *F* and *T* of BW and PW were 1.38%, 1.56 × 10^6 J m^−3, 1.67% and 1.09 × 10^6 J m^−3 (Table 1). By contrast, the bamboo possessed a strong *F* of 2.49–2.42% and *T* of 2.03–5.11 × 10^6 J m^−3, which meant that the bamboo endured much more plastic deformation followed by delayed failure after it fractured. The *F* value of bamboo was at least 1.8 times that of wood, while the average *T* (3.57 × 10^6 J m^−3) of bamboo was 2.28 times that of BW and 3.27 times of PW in Fig. 6b–c. Therefore, it can be said that bamboo had a higher *F* and *T* than wood with the same density. The research of Obataya et al. [11] observed that the excellent flexural properties of bamboo were attributed to the perfect combination of fiber and parenchyma cells. All of these results indicated that bamboo could be used more as natural structural materials than wood of the same size due to it having a greater toughness and more flexibility; such as in BWCPs.

3.3.2. *Comparison on microstructures and toughening mechanisms*

The difference of in the microstructure between moso bamboo and the control wood samples structure in the cross section, is in the cell morphologies and arrangement; which

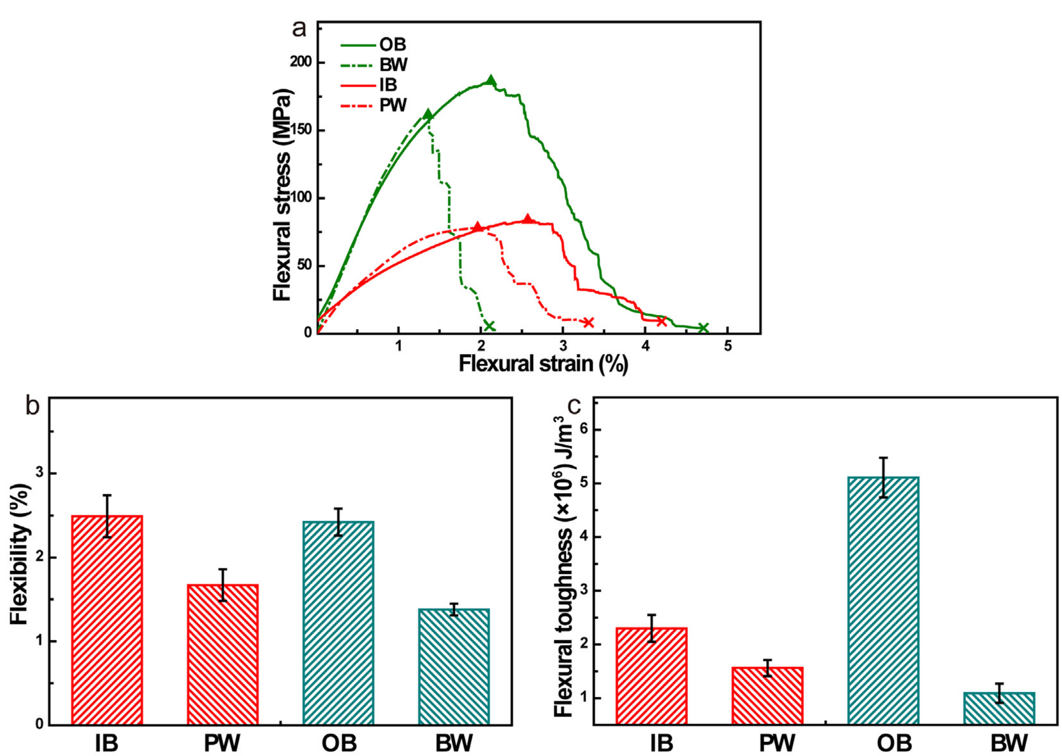

Fig. 6 – Comparison of flexural behaviors between bamboo and wood with similar density. (a) Typical flexural stress–strain curves of bamboo (IB and OB) and wood (BW and PW); (b) the flexibility of bamboo and wood; (c) the flexural toughness of bamboo and wood.

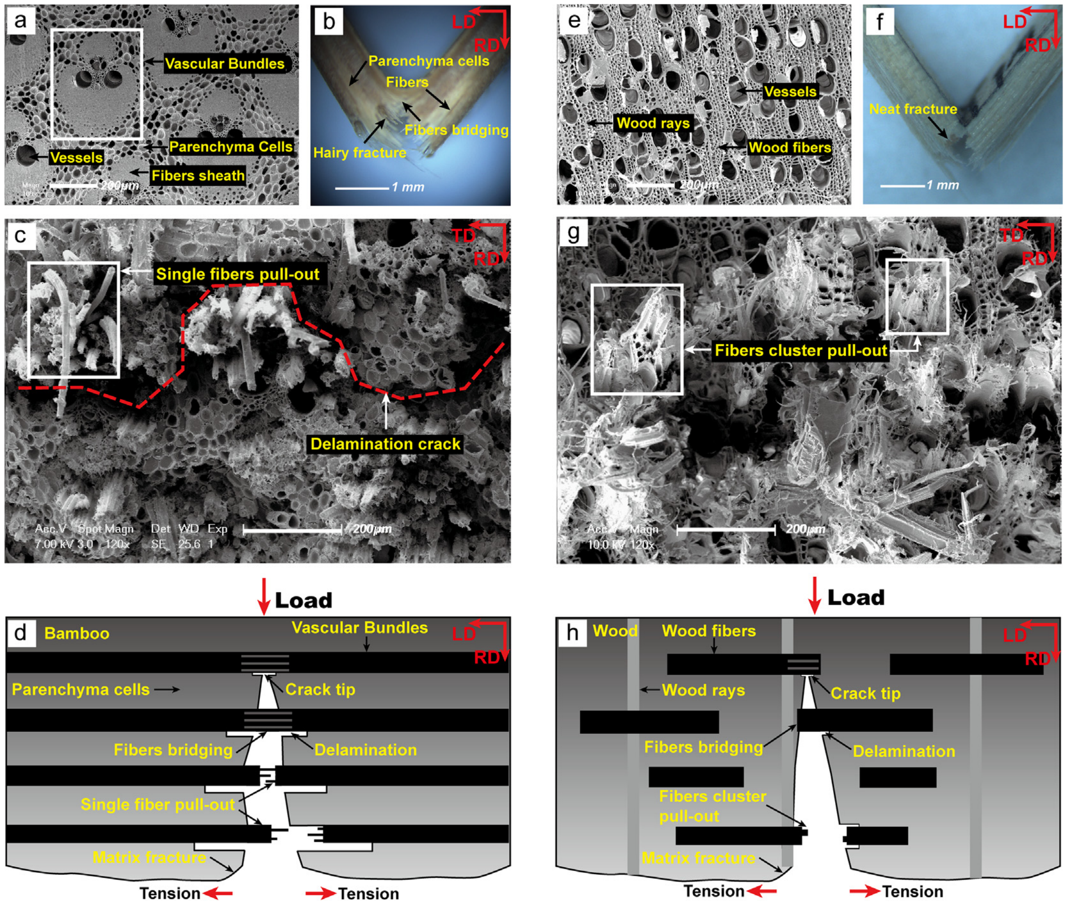

Fig. 7 – The difference of microstructure and fracture morphology between moso bamboo and poplar wood PW (similar to the Birch wood (BW) in anatomy). The microstructure of (a) moso bamboo and (e) poplar wood in the cross section; The fracture morphology on the axial direction for bamboo (b) and wood (f); The fracture morphology of bamboo (c) and wood (g) on the cross section; Effects of cells structure on the flexural fracture behaviors and toughening mechanisms within bamboo (d) and wood (h).

eventually leads to significantly different flexibility and flexural toughness. Macroscopically, bamboo is a typical natural material with unidirectional hard vascular bundles that are reinforced by soft foamy parenchyma cells, where they function as a buffer when bamboo undergoes compressive stress and deformation (Fig. 7a); the wood structure on the other hand has radial wood rays crisscrossed with the axial wood fibers, which ensures higher flexural modulus (stiffness) of wood but also limited its *F* and flexural strength in (Fig. 7e).

In addition to acting on the flexibility before the fracture point, the differences in the microstructure also played a role in the failure mechanism. Crack deflection, fibers bridging, and pull-out were the main toughening mechanisms observed in bamboo (Fig. 7d). When cracks initiated in the parenchyma cells at the bottom of the samples they flowed through the vessels, vascular bundles, and parenchyma cells during the flexural fracture along the radial direction (RD). The broken parenchyma cells caused elevation differences due to the fiber pulled-out, which resulted in a hairy fracture morphology at the macro level on the axial surface (Fig. 7b). Multi-scale fiber pull-out was observed in the cross-section (Fig. 7c), which included the pull-out of vascular bundles and long individual fibers from broken vascular bundles [5]. Delamination cracks occurred in the plain of the parenchyma cells at a microlevel, where the crack propagation path moved through the porous parenchyma cells and tough fibers (Fig. 7c) [31,40]. Cracks within the parenchyma cells along the RD propagated in the weaker interface of the fibers/parenchyma cells where they along the longitudinal direction (LD), where upon encountering vascular bundles, they would form into delamination cracks (Fig. 7d); which has been considered one of the main toughening mechanisms induced by high yield strength in ultra-strong steel [41]. To analyze the influence of exhibited by cracks on their reduction as a driving force for propagation in both the RD and LD (Fig. 7d), the local effective stress intensity factor (K_{eff}) at the crack tip can be approximately calculated by Hanlon et al. [42]:

$$K_{eff} = \cos^2(\theta/2)K_I \quad (7)$$

where the stress intensity factor of straight crack growth (K_I) and the crack deflection angle (θ) were used. Due to the interface and shape of various types of cells, crack deflection angle in the parenchyma cells (θ_p) and fibers (θ_f) was 25–60° and 45–60° in the RD, and 80–90° and 60–90° in the LD [4]. The

K^{p}_{eff} and K^{f}_{eff} were estimated to be (0.75–0.95) K_I and (0.75–0.85) K_I in the RD, and (0.6–0.75) K_I and (0.5–0.75) K_I in the LD. It was observed that the crack deflection can effectively reduce K_I, especially the deflection in parenchyma cells and fibers along the LD from the RD. Due to the lower stress intensity factors (K_{eff}) of bamboo's respective cells, the combined effect reduces the driving force of crack propagation in the overall bamboo structure.

The neat morphologies on the longitudinal surface were found for the flexural fractured wood PW (Fig. 7f). The wood fibers broke into short fibers clusters followed by pull out from the wood cells matrixes (Fig. 7g), which showed less obvious pull-out during the fracture process. Cracks in the PW propagated along the weak interface between the wood rays and cells matrixes, only a few radial cracks were deflected to the LD to form delamination cracks in the woods cross section (Fig. 7h). Therefore, the phenomena above confirmed that the toughening effect of wood fibers was lower than that of bamboo fibers at the macrolevel (Fig. 6 and Table 1).

The bamboo and wood exhibit different fiber pull-out lengths and fracture aggregation states. In order to further analyze the effect of the fiber pull-out on the energy dissipation process, a single fiber pull-out model was used (Eq. (8)):

$$P = \pi D l_e \tau \quad (8)$$

where P is pull-out force, D is the diameter of single fiber, l_e is the length of the fiber embedded in the parenchyma cells matrixes, τ is the shear strength of interface between fibers and parenchyma cells matrixes. To completely pull out the broken fiber with length of l_e after bridging from the parenchyma cells matrixes and adjacent fibers, huge frictional resistance must be overcome, thus, the pull-out energy (Ep) was expressed as: (Eq. (9)):

$$Ep = P \times l_e = \pi D l_e^2 \tau \quad (9)$$

With similar fibers diameter and shear strength of fibers/cells matrixes to wood, the longer pull-out fibers in bamboo made an outstanding contribution to its toughness, which costs considerable energy ($P \times l_e$) to pull out long fibers from bamboo compared to fibers cluster from wood [43]. This was confirmed by the flexural test results (Fig. 6), where the bamboo with longer fiber pull-out length displayed higher flexural toughness.

This difference in fibers pull-out length between bamboo and wood was related to their mechanical properties, aspect ratio, microfibrils angle (MFA). Previous research had shown that the tensile modulus, strength, and aspect ratio of bamboo single fiber were 26 GPa, 1685 MPa, and 122–165, respectively; which were higher than that of wood fiber (14 GPa, 908 MPa and about 60) [44,45]. Cracks were caused to deflect to the cells interface when they encountered the bamboo fiber instead of breaking them due to the fiber's higher performance and slender shape and when breakage did occur there was pull out. Wood fibers were more easily broke into short fibers clusters. In addition, higher aspect ratio of fibers promoted stress transfer between fiber and parenchyma cells matrixes through the interface; which helped enhance the overall F and T of bamboo. Lastly, the microfibrils angle (MFA) of bamboo and wood was tested in order to compare and analyze the effect on flexural toughness. The X-ray diffraction pattern of microfibrils in the cell wall and the MFA of bamboo, PW, and BW were calculated to be 11.1°, 14.8°, and 13.6° (Fig. 8). The greater the angle formed by reinforcing microfibrils with the cell axis (along with the applied force direction). The greater the normal load (shear) on the cell wall, caused the interface between the fibrils and the LCC matrixes to be pulled apart which accelerated the destruction of the cells wall.

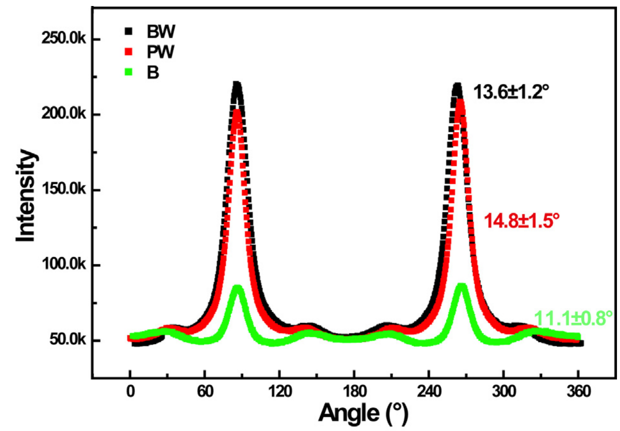

Fig. 8 – X-ray diffraction spectrum of bamboo (B), popular wood (PW) and Birch wood (BW) in microfibrils angle (MFA) measurement.

In the context of the scarcity of wood resources, bamboo is the only alternative to wood applications in traditional fields, such as wood construction, woody panels, and wood-based composites [46]. The BWCP is a sustainable composite product that makes full use of bamboo's unique characteristics—high flexibility and flexural toughness. These characteristics are of great significance to the development of the bamboo industry, including bamboo weaving crafts, and curved bamboo furniture.

4. Conclusion

An original approach was established to quantitatively evaluate the bamboo's flexibility and flexural toughness simultaneously. Aiming at the gradient distribution and aggregate structure of fibers on natural moso (*P. edulis*) bamboo, the investigation results showed that the flexibility of bamboo decreased but the flexural strength and toughness increased with the increase of fibers contents from the inner to outer layers. Bamboo possesses both high strength and high toughness due to the high content of fibers, however a conflict between flexibility and flexural toughness is derived from the reverse distribution of parenchyma cells and fibers. Anatomically, the asymmetric aggregate structure (vascular bundles) of fibers in the outer layer of bamboo is the main reason for the difference in flexibility and flexural toughness under bending direction and that asymmetric difference gradually disappeared when approaching the inner layer due to the substantially symmetrical structure of vascular bundles. Comparison between bamboo and wood at similar densities demonstrated that the flexibility of bamboo was at least 1.8 times that of wood, while the average flexural toughness of bamboo was 1.42–3.46 times that of the *B. alnoides* and 2.03–4.96 times that of poplar wood. Compared with the crisscross cells in wood, the combination of high-performance fibers and foamy parenchyma cells was the key to bamboo's flexibility, while its excellent flexural toughness was stemmed out from the fiber bridging and pull-out caused by its high performance, aspect ratio, low microfibrils angle (MFA), and crack deflection along the longitudinal/radial direction (LD/RD) compared with wood of similar densities. These studies on bamboo could make it an attractive choice as a green material for sustainable construction, especially for optimizing existing process of bamboo-based winding composites pipes (BWCPs).

Declaration of Competing Interest

The authors declare that they have no known competing financial interests or personal relationships that could have appeared to influence the work reported in this paper.

Acknowledgement

This research was funded by the National Natural Science Foundations of China (31770598). The authors would also like to thank Fujian Youzhu Technology Co., Ltd. for supplying the raw bamboo materials.

REFERENCES

[1] Paraskeva T, Grigoropoulos G, Dimitrakopoulos E. Design and experimental verification of easily constructible bamboo footbridges for rural areas. Eng Struct 2017;143:540–8. https://doi.org/10.1016/JengStruct2017.04.044.
[2] Wei X, Wang G, Smith L, Jiang H. The hygroscopicity of moso bamboo (Phyllostachys edulis) with a gradient fiber structure. J Mater Res Technol 2021;15:4309–16. https://doi.org/10.1016/j.jmrt.2021.10.038.
[3] Fu Y, Fang H, Dai F. Study on the properties of the recombinant bamboo by finite element method. Compos Part. B 2017;115:151–9. https://doi.org/10.1016/Jcompositesb.2016.10.022.
[4] Habibi K Meisam, Lu Yang, Latella B. Crack Propagation in Bamboo's Hierarchical Cellular Structure. Sci Rep 2014;4:5598. https://doi.org/10.1038/srep05598.
[5] Chen G, Luo H, Yang H, Zhang T, Li S. Water effects on the deformation and fracture behaviors of the multi-scaled cellular fibrous bamboo. Acta Biomater 2017;65:203–15. https://doi.org/10.1016/Jactbio.2017.10.005.
[6] Deng J, Wang G. Axial tensile properties and flexibility characteristics of elementary units from multidimensional bamboo-based composites: radial and tangential moso bamboo slivers. Holzforschung 2018;72:779–87. https://doi.org/10.1515/hf-2018-0017.
[7] Wu Y, Zheng Y, Yang F, Yang L. Preparation process and characterization of mechanical properties of twisted bamboo spun fiber bundles. J Mater Res Technol 2021;14:2131–9. https://doi.org/10.1016/j.jmrt.2021.07.080.
[8] Chen F, Li M, Xin W, Zhou H, Smith L, Wang G, et al. Development of bamboo winding composite pipe (BWCP) and its compression properties. Bioresources 2019;14(3):5875–82.
[9] Chele E, Ricardo M, Ana P, Teresa M. Bamboo from traditional crafts to contemporary design and architecture. Procedia Soc Behav Sci 2012;51:777–81. https://doi.org/10.1016/Jsbspro.2012.08.239.
[10] Getu D, Nallamothu R, Masresha M, Nallamothu S, Nallamothu A. Production and characterization of bamboo and sisal fiber reinforced hybrid composite for interior automotive body application. Mater Today Proc 2021;38:2853–60. https://doi.org/10.1016/Jmatpr.2020.08.780.
[11] Obataya E, Kitin P, Yamauchi H. Bending characteristics of bamboo (Phyllostachys pubescens) with respect to its fiber–foam composite structure. Wood Sci Technol 2007;41:385–400. https://doi.org/10.1007/s00226-007-0127-8.
[12] Mannan S, Parameswaran V, Basu S. Stiffness and toughness gradation of bamboo from a damage tolerance perspective. Int J Solid Struct 2018;143:274–86. https://doi.org/10.1016/Jijsolstr.2018.03.018.
[13] Wei X, Chen F, Wang G. Flexibility characterization of bamboo slivers through winding-based bending stiffness method. J Forestry Eng 2020;5:48–53. https://doi.org/10.13360/j.issn.2096-1359.201905046 (in Chinese).
[14] Krause J, Silva F, Ghavami K, Gomesbc O, Filhod R. On the influence of Dendrocalamus giganteus bamboo microstructure on its mechanical behavior. Construct Build Mater 2016;127:199–209. https://doi.org/10.1016/Jconbuildmat.2016.09.104.
[15] Sharma B, Harries K, Ghavami K. Method of determining transverse mechanical properties of full-culm bamboo. Construct Build Mater 2013;38:627–37. https://doi.org/10.1016/Jconbuildmat.2012.07.116.
[16] Grosser D, Liese W. On the anatomy of Asian bamboos with special reference to their vascular bundles. Wood Sci Technol 1971;5:290–312. https://doi.org/10.1007/BF00365061.
[17] Kanzawa E, Aoyagi S, Nakano T. Vascular bundle shape in cross-section and relaxation properties of moso bamboo (*phyllostachys pubescens*). Mater Sci Eng C 2011;31:1050–4. https://doi.org/10.1016/Jmsec.2011.03.004.
[18] Wei X, Zhou H, Chen F, Wang G. Bending flexibility of moso bamboo (*phyllostachys edulis*) with functionally graded structure. Materials 2019;12:2007. https://doi.org/10.3390/ma12122007.
[19] Palombini F, Mariath J, Oliveira B. Bionic design of thin-walled structure based on the geometry of the vascular bundles of bamboo. Thin-Walled Struct 2020;155:106936. https://doi.org/10.1016/Jtws.2020.106936.
[20] Silva E, Walters M, Paulino G. Modeling bamboo as a functionally graded material: lessons for the analysis of affordable materials. J Mater Sci 2006;41:6991–7004. https://doi.org/10.1007/s10853-006-0232-3.
[21] Wegst U. Bending efficiency through property gradients in bamboo palm and wood-based composites. J Mech Behav Biomed Mater 2011;4(5):744–55. https://doi.org/10.1016/Jjmbbm.2011.02.013.
[22] Dixon P, Gibson L. The structure and mechanics of Moso bamboo material. J R Soc Interface 2011;11(99):20140321. https://doi.org/10.1098/rsif.2014.0321.
[23] Youssefian S, Rahbar N. Molecular origin of strength and stiffness in bamboo fibrils. Sci Rep 2015;5:11116. https://doi.org/10.1038/srep11116.
[24] Tan T, Rahbar N, Allameh S, Kwofie S, Dissmore D, Ghavami K, et al. Mechanical properties of functionally graded hierarchical bamboo structures. Acta Biomater 2011;7:3796–803. https://doi.org/10.1016/Jactbio.2011.06.008.

[25] Hao H, Tam L, Lu Y, Lau D. An atomistic study on the mechanical behavior of bamboo cell wall constituents. Composer Part B 2018;151:222–31. https://doi.org/10.1016/Jcompositesb.2018.05.046.
[26] Chen M, Liu R, Wang G, Fang C, Ma X, Zhang S, et al. Parenchyma cell morphological changes of bamboo under bending. Sci Silvae Sin 2020;56:142–7. https://doi.org/10.11707/j.1001-7488.20200216 (in Chinese).
[27] Wang Y, Liu C, Zhao R, McCord J, Rials T, Wang S. Anatomical characteristics microfibril angle and micromechanical properties of cottonwood (*populus deltoides*) and its hybrids. Biomass Bioenergy 2016;93:72–7. https://doi.org/10.1016/Jbiombioe.2016.06.011.
[28] Chen G, Luo H, Wu S, Guan J, Luo J, Zhao T. Flexural deformation and fracture behaviors of bamboo with gradient hierarchical fibrous structure and water content. Compos Sci Technol 2018;157:126–33. https://doi.org/10.1016/Jcompscitech.2018.01.034.
[29] Wang D, Lin L, Fu F. Fracture mechanisms of moso bamboo (*phyllostachys pubescens*) under longitudinal tensile loading. Ind Crop Prod 2020;153:112574. https://doi.org/10.1016/Jindcrop.2020.112574.
[30] Cave I. Theory of X-ray measurement of microfibril angle in wood. Wood Sci Technol 1997;31:225–34. https://doi.org/10.1007/BF00702610.
[31] Habibi M, Samaei A, Gheshlaghi B, Lu J, Lu Y. Asymmetric flexural behavior from bamboo's functionally graded hierarchical structure: underlying mechanisms. Acta Biomater 2015;16:178–86. https://doi.org/10.1016/Jactbio.2015.01.038.
[32] Shao Z, Wang F. The fracture mechanics of plant materials: wood and bamboo. German: Springer; 2018. https://doi.org/10.1007/978-981-10-9017-2.
[33] Amada S, Ichikawa Y, Munekata T, Nagase Y, Shimizu H. Fiber texture and mechanical graded structure of bamboo. Compos B Eng 1997;28(1–2):13–20. https://doi.org/10.1016/S1359-8368(96)00020-0.
[34] Ritchie R. The conflicts between strength and toughness. Nat Mater 2011;10:817–22. https://doi.org/10.1038/nmat3115.
[35] Jiang Z. Bamboo and rattan in the world. Beijing: China Forestry Pub. House; 2007.
[36] Wegst U, Bai H, Saiz E, Tomsia A, Ritchie R. Bioinspired structural materials. Nat Mater 2014;14:23–36. https://doi.org/10.1038/nmat4089.
[37] Iqbal S, Khan R. Effect of brushing & abrading of laminae on the mode I fracture toughness of glass fiber/epoxy composite. Construct Build Mater 2020;261:120508. https://doi.org/10.1016/Jconbuildmat.2020.120508.
[38] Suzuki M, Saruwatari K, Kogure T, Yamamoto Y, Nishimura T, Kato T, et al. An acidic matrix protein pif is a key macromolecule for nacre formation. Science 2019;325:1388–90. https://doi.org/10.1126/science.1173793.
[39] Lu K. Making strong nanomaterials ductile with gradients. Science 2014;345:1455–6. https://doi.org/10.1126/science.1255940.
[40] Taylor D. Measuring fracture toughness in biological materials. J Mech Behav Biomed Mater 2018;77:776–82. https://doi.org/10.1016/Jjmbbm.2017.07.007.
[41] Liu L, Yu Q, Wang Z, Jon E, Huang M, Ritchie R. Making ultrastrong steel tough by grain-boundary delamination. Science 2020;368(6497):1347–52. https://doi.org/10.1126/science.aba9413.
[42] Hanlon T, Tabachnikova E, Suresh S. Fatigue behavior of nanocrystalline metals and alloys. Int J Fatig 2005;27:1147–58. https://doi.org/10.1016/Jijfatigue.2005.06.035.
[43] Smith B, Schäffer T, Viani M, Thompson J, Frederick N, Kindt J, et al. Molecular mechanistic origin of the toughness of natural adhesives fibres and composites. Nature 1999;399:761–3. https://doi.org/10.1038/21607.
[44] Wang G, Shi S, Wang J, Yu Y, Cao S, Cheng H. Tensile properties of four types of individual cellulosic fibers. Wood Fiber Sci 2011;43(4):353–64.
[45] Tian G. The main influence factors of bamboo fiber mechanical properties. PhD Thesis. Beijing: Chinese Academy of Forestry China; 2015.
[46] Verma C, Sharma N, Chariar V, Maheshwari S, Hada K. Comparative study of mechanical properties of bamboo laminae and their laminates with woods and wood based composites. Composer Part B 2014;60:523–30. https://doi.org/10.1016/Jcompositesb.2013.12.061.